Development 126, 13-21 (1999)
Printed in Great Britain © The Company of Biologists Limited 1998
DEV2351

Gli3 (*Xt*) and *formin* (*ld*) participate in the positioning of the polarising region and control of posterior limb-bud identity

Aimée Zúñiga and Rolf Zeller*

EMBL, Meyerhofstrasse 1, D-69117 Heidelberg, Germany
Present address of both authors: Department of Developmental Biology, University of Utrecht, Padualaan 8, 3584 CH Utrecht, The Netherlands
*Author for correspondence (e-mail: R.Zeller@Bio.UU.NL)

Accepted 16 October; published on WWW 3 December 1998

SUMMARY

During initiation of limb-bud outgrowth in vertebrate embryos, the polarising region (limb-bud organizer) is established upon activation of the Sonic Hedgehog (SHH) signaling molecule at the posterior limb-bud margin. Another hallmark of establishing anteroposterior limb-bud identities is the colinear activation of HoxD genes located at the 5′ end of the cluster (5′HoxD genes). The unique and shared functions of *Gli3* and *formin* in these determinative events were genetically analyzed using single and double homozygous *Extra-toes (Xt*; disrupting *Gli3*) and *limb deformity* (*ld*; disrupting *formin*) mouse embryos. Analysis of the limb skeletal phenotypes reveals genetic interaction of the two genes. In addition to loss of digit identity and varying degrees of polydactyly, proximal skeletal elements are severely shortened in *Xt;ld* double homozygous limbs. The underlying molecular defects affect both establishment of the polarising region and posterior limb-bud identity. In particular, the synergism between *Gli3*- and *formin*-mediated mesenchyme-AER interactions positions the SHH signaling center at the posterior limb-bud margin. The present study shows that establishment and positioning of the polarising region is regulated both by restriction of *Shh* through *Gli3* and its positive feedback regulation through *formin*. Concurrently, *Gli3* functions independently of *formin* during initial posterior nesting of 5′HoxD domains, whereas their subsequent distal restriction and anterior expansion depends on genetic interaction of *Gli3* and *formin*.

Key words: Mouse mutant, HoxA, HoxD, Limb bud, Patterning, Posterior limb identity, *Shh* activation

INTRODUCTION

Growth and patterning of vertebrate limb buds is controlled by epithelial-mesenchymal interactions of two main signaling centers. Apical ectodermal ridge (AER) signals promote outgrowth and maintain the posterior mesenchymal cells of the polarising region in an active state. The polarising region functions as a mesenchymal organizer expressing the Sonic Hedgehog (SHH) signaling molecule (reviewed by Cohn and Tickle, 1996; Johnson and Tabin, 1997). SHH signaling controls growth and patterning of distal limb structures including the autopod (digits; Riddle et al., 1993; Chiang et al., 1996). However, establishment of polarizing activity in the presumptive limb field long precedes *Shh* activation (Hornbruch and Wolpert, 1991). Experimental evidence indicates that combinations of Hox genes expressed by the flank mesenchyme position the presumptive limb field (Cohn et al., 1997) and that retinoid signaling induces polarizing activity (Lu et al., 1997; Stratford et al., 1997). In particular, *Hoxb8* marks polarizing activity in the forelimb field and seems to participate in induction of SHH signaling during onset of limb-bud outgrowth (Charité et al., 1994). Furthermore, a positively acting AER factor has also been implicated in *Shh* activation (Grieshammer et al., 1996; Helms et al., 1996; Ros et al., 1996), but the mechanisms restricting *Shh* activation to the posterior limb-bud margin remained unknown.

Proliferation and commitment of limb-bud mesenchymal progenitors seem largely determined by differential expression of Hox genes located at the 5′ ends of the HoxA and HoxD clusters. For example, genetic analysis revealed both unique and redundant functions for paralogous 5′HoxA and 5′HoxD genes during limb-bud morphogenesis, which correlate well with distinct and overlapping distributions in limb buds (reviewed by Duboule, 1995; Johnson and Tabin, 1997). During the limb field to limb-bud transition, colinear activation of 5′HoxD genes results in their posteriorly restricted, nested early expression domains. During subsequent limb-bud outgrowth, the 5′HoxD domains expand anterior within the distal mesenchyme (late domains; reviewed by Duboule, 1992). These late 5′HoxD domains control formation of the autopod as indicated by genetic and evolutionary studies (Dollé et al., 1993; Sordino et al., 1995).

Analysis of classical mouse mutations has proven helpful in understanding the genetic hierarchies that control determinative steps during vertebrate limb pattern formation (reviewed by Niswander, 1997). In particular, alleles of the

haploinsufficient mouse *Extra-toes* (*Xt*) mutations (Johnson, 1967) disrupt the *Gli3* gene (Hui and Joyner, 1993; Schimmang et al., 1992) and mutations in its human homologue cause several distinct genetic disorders. All known mutations in both human and mouse *Gli3* genes affect limb morphogenesis among other developmental processes (reviewed by Biesecker, 1997). The polydactyly of *Xt* homozygous (*Xt/Xt*) limbs was interpreted as being caused by induction of an ectopic anterior SHH cascade (polarizing activity) which in turn leads to anterior ectopic 5′HoxD expression during hand plate formation (Masuya et al., 1995; Buescher et al., 1997). Activation of *Gli3* in the limb field slightly precedes initiation of limb-bud outgrowth and persists in all limb mesenchymal cells with exception of *Shh*-expressing cells (Marigo et al., 1996; Masuya et al., 1997). Their mutually exclusive distribution and the repression of *Gli3* by retrovirus-mediated ectopic *Shh* in chicken limb buds led to the proposal that *Gli3* and SHH repress one another (Masuya et al., 1995; Marigo et al., 1996).

In contrast, several recessive and most likely hypomorphic alleles of the mouse *limb deformity* (*ld*) mutation disrupt the *formin* gene (Maas et al., 1990; Woychik et al., 1990) and alter the patterning of distal limb skeletal elements, resulting in fusion and loss of digits (syndactyly). The positive SHH/FGF-4 feedback loop, controlling morphogenesis of distal limb structures (Laufer et al., 1994; Niswander et al., 1994) is disrupted in *ld* homozygous (*ld/ld*) limb buds, which results in reduced polarising activity (Chan et al., 1995; Haramis et al., 1995; Kuhlman and Niswander, 1997). This disruption is due to a primary mesenchymal defect (Kuhlman and Niswander, 1997) preventing complete differentiation of the AER (Zeller et al., 1989) and the induction of *Fgf-4* in the posterior AER. Taken together these studies establish that mesenchymal *formin* functions primarily in establishment of the signalling interactions between the polarizing region (SHH) and the AER (FGF-4). Most likely as a consequence of disrupting these mesenchyme-AER interactions, the transition from early to late 5′HoxD domains is delayed in *ld/ld* limb buds (Haramis et al., 1995). Consistent with a genetic function in establishing the SHH/FGF-4 feedback loop, *formin* is expressed by posterior and distal limb-bud mesenchymal cells (Trumpp et al., 1992; Chan et al., 1995). High levels of *formin* transcripts are also expressed by the AER during early limb-bud outgrowth, but transgene-mediated *formin* re-expression in the *ld* mutant AER fails to rescue the SHH/FGF-4 feedback loop and limb-bud patterning (A. G. Haramis, D. James, K. Brennan and R. Zeller, unpublished data). Furthermore, targeted disruption of the predominant *formin* isoform in the AER does not disrupt limb morphogenesis (Wynshaw-Boris et al., 1997). These studies agree with those of Kuhlman and Niswander (1997) and strengthen the conclusion that only mesenchymal *formin* is essential to establish the SHH/FGF-4 feedback loop.

Possible interactions and/or unique functions of *Gli3* and *formin* during early limb-bud patterning were genetically studied by comparative analysis of both single and *Xt;ld* (*Xt/Xt;ld/ld*) double homozygous embryos. Our studies show that *Gli3* functions initially independent of *formin* to posteriorly restrict 5′HoxD genes during onset of limb-bud outgrowth. In contrast, concurrent positioning and establishment of the *Shh*-expressing polarising region at the posterior limb-bud margin is controlled by a synergistic genetic interaction of *Gli3* and *formin*. Transacting *Gli3* and *formin* also regulate aspects of the transition from early to late 5′HoxD domains and of the differential distribution of 5′HoxD from 5′HoxA paralogues.

MATERIALS AND METHODS

Genetic crosses and genotyping of embryos

Previous analysis of the *ld* limb-bud phenotype established that different *ld* alleles disrupt the SHH/FGF-4 signaling feedback loop in the same way (Haramis et al., 1995; Chan et al., 1995). Therefore, the ld^{In2} allele was used because the genotypes can be easily determined by PCR (see below). All strains were maintained in a mixed C57Bl6/SJL F_1 background. Two alleles of the *Xt* mutation were used: in the Xt^J allele, the 3′ part of the *Gli3* gene is deleted (Hui and Joyner, 1993), whereas the 5′ part of the *Gli3* open reading frame is deleted in the Xt^H allele (Schimmang et al., 1992). Both *Xt* alleles display identical polydactylous limb phenotypes in homozygous embryos (Hui and Joyner, 1993). Therefore, most analysis was performed by intercrossing ld^{In2} mutant mice with the Xt^J strain, as offspring can easily be PCR genotyped using genomic DNA isolated from embryonic heads (Haramis et al., 1995; Buescher et al., 1997). However, all results were confirmed by also analyzing ld^{In2}/Xt^H intercrosses. No molecular differences were detected between limb buds of the following genotypes: wild-type (*+/+;+/+*), *Xt/+;ld/+*, *Xt/+;+/+* and *+/+;ld/+*. Therefore, these genotypes were considered phenotypically wild type in agreement with previous studies detecting ectopic *Shh* only in *Xt/Xt* limb buds (Buescher et al., 1997). Similarly, no differences were detected between *Xt/Xt;+/+* and *Xt/Xt;ld/+* or *ld/ld;+/+* and *ld/ld;Xt/+* limb buds.

Age-matching of embryos

ld/+;Xt/+ females were crossed with either *ld/+;Xt/+* or *ld/ld;Xt/+* males to obtain single and double mutant litter mates. The day of vaginal plug detection is defined as embryonic day zero and embryos were age-matched by somite numbers (variation: ±2 somites; see Haramis et al., 1995).

Skeletal preparations

Due to perinatal lethality of both *Xt/Xt* (Johnson, 1967) and *Xt;ld* double homozygous embryos, the pattern of limb skeletal elements was analyzed during embryonic day E15, the oldest developmental stages at which these genotypes were recovered at expected ratios. Embryos were stained for cartilage and bones using standard Alcian blue and Alizarin red staining.

Whole-mount in situ hybridization

Whole-mount in situ hybridization (Haramis et al., 1995) was performed using the following probes: *Shh* (Echelard et al., 1993), *Hoxa11* and *Hoxa13* (Small and Potter, 1993), *Hoxd9* to *Hoxd13* (Dollé et al., 1989), *Hoxb8* (Charité et al., 1994), *Ptc* (Platt et al., 1997), *Gli3* (Buescher et al., 1997) and *Gli* (Hui et al., 1994). *Formin* transcripts were detected using a riboprobe complementary to their 3′ part (1.7 kb *Stu*I-*Eco*RI probe, Woychik et al., 1990). For comparative studies, embryos were always hybridized in the same experiment to avoid variation. Reproducibility of all results was established by analyzing several embryos in independent experiments.

RESULTS

Xt;ld double homozygous limbs display a loss of digit identity and truncations of proximal skeletal elements

Possible direct dependence of *formin* on *Gli3* (and vice versa) was examined by studying the distribution of *formin* transcripts

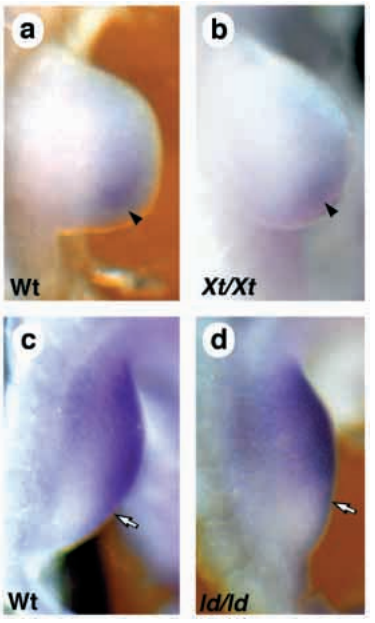

Fig. 1. Mesenchymal *formin* distribution in *Xt/Xt* mutant and *Gli3* expression in *ld/ld* mutant limb buds are not affected at embryonic day 10.5 (35 somites). (a,b) *Formin* expression in the forelimb-bud mesenchyme of a wild-type (a) and *Xt/Xt* (b) embryo. In both genotypes, expression is highest in posterior-distal mesenchymal cells (arrowheads) and decreases towards the anterior in the distal mesenchyme. (c,d) *Gli3* expression in hindlimb buds of wild-type (c) and *ld/ld* (d) embryos. *Gli3* expression is excluded from posterior mesenchyme (arrows).

in *Xt/Xt* and *Gli3* transcripts in *ld/ld* limb buds. Fig. 1 shows that no significant alterations of *formin* transcripts are detected by comparing wild type (Fig. 1a) to *Xt/Xt* mutant limb buds (Fig. 1b). Despite the fact that *Shh* expression is not upregulated in *ld/ld* limb buds (Chan et al., 1995; Haramis et al., 1995; Kuhlman and Niswander, 1997), *Gli3* remains excluded from posterior limb-bud mesenchyme in both wild-type (Fig. 1c; see also Masuya et al., 1997) and *ld/ld* limb buds (Fig. 1d). During the developmental stages relevant to this study (prior to embryonic day 11, see below), neither *formin* nor *Gli3* expression is directly affected in either *Xt/Xt* or *ld/ld* limb buds, respectively.

Possible synergistic genetic interactions of *formin* and *Gli3* were uncovered by analyzing the limb phenotypes of *Xt;ld* double homozygous embryos (Fig. 2). Wild-type mouse limbs of embryonic day 15 have five distinct digits (Fig. 2a), whereas *ld/ld* limbs are syndactylous (Fig. 2b; see also Woychik et al., 1985). In contrast, *Xt/Xt* limbs display varying degrees of preaxial polydactyly and associated loss of digit identities (Fig. 2d,e; see also Johnson, 1967). Only rudimentary digits form in *Xt;ld* double homozygous limbs (Fig. 2g,h). The autopods of such limbs often display partial polydactyly and syndactyly (Fig. 2g). Their rudimentary digits lack phalanges, which indicates that coordinated outgrowth and patterning of distal limb skeletal elements are affected, resulting in autopods with apparently little (Fig. 2g) or no discernible anteroposterior polarity (Fig. 2h). Most strikingly, the stylopods are always severely reduced (humerus, white arrowhead, Fig. 2i; femur, not shown) and an enlarged foramen is present in the scapula of all *Xt;ld* double homozygous limbs (black arrowhead in Fig. 2i). In addition, ossification of all skeletal elements is always severely delayed as only a single ossification center has formed by this developmental stage (compare arrows, Fig. 2i to c,f).

Gli3 controls initial posterior restriction of the 5′HoxD domains in limb buds independent of *formin*

Sequential activation of 5′HoxD genes results in their distinct, posteriorly nested early expression domains in wild-type limb

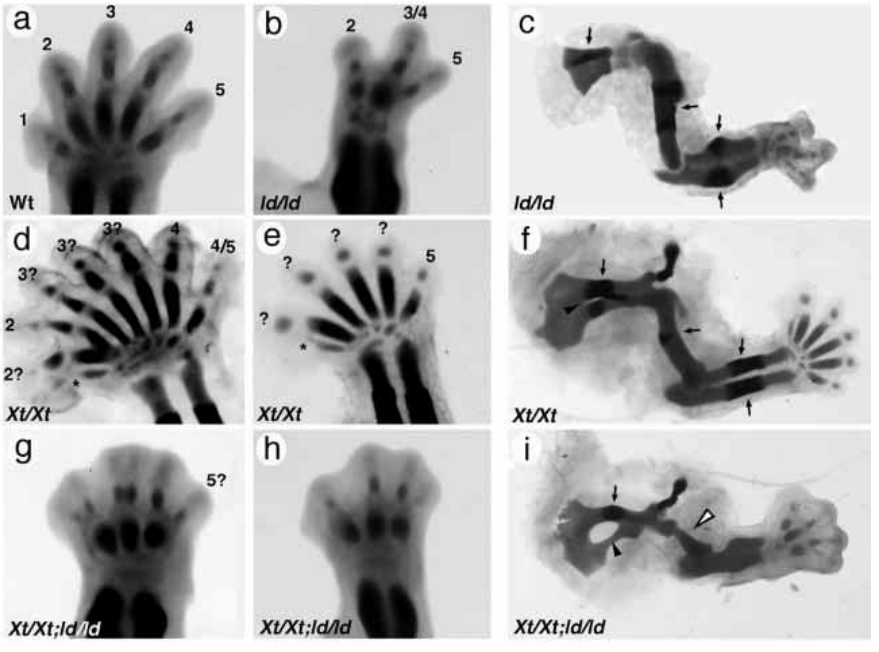

Fig. 2. Limb skeletal phenotypes at embryonic day 15.5. (a) Wild-type forelimb. Digits are numbered **1** to **5** with anterior to posterior polarity. (b) *ld* homozygous forelimb. Digit **1** is missing and digits **3** and **4** are fused. (c) *ld/ld* forelimb with characteristic fusion of ulna and radius. (d,e) Two different *Xt/Xt* forelimbs to illustrate the variable loss of anteroposterior digit identities. (d) Preaxial polydactyly with associated loss of digit **1**. Numbers refer to the presumed digit identities, which are based on phalange numbers and morphology. (e) Brachydactyly. Apart from digit **5**, all digits appear identical and lack phalanges. Interdigital webbing is observed. Asterisks in d,e mark isolated cartilage condensations. (f) *Xt/Xt* forelimb. 40% of all limbs analyzed show a scapula with an incompletely fused foramen (black arrowhead). (g,h) Two *Xt;ld* double homozygous forelimbs to illustrate the range of autopod phenotypes. Varying numbers of rudimentary digits without distinct identity and lacking phalanges form. (g) Six partially fused and (h) four distinct condensations; phalanges and metacarpals appear very rudimentary and are often fused. The resulting autopod appears often rather symmetrical and extensive interdigital webbing is apparent. (i) *Xt;ld* double mutant forelimb. The scapula is always incompletely fused (black arrowhead), the humerus is drastically shortened (white arrowhead) and ulna and radius are fused similarly to *ld/ld* forelimbs (compare to (c)). Black arrows in c,f,i indicate ossification centers.

buds (Fig. 3a,e; reviewed by Duboule, 1992). These early 5′HoxD domains are correctly established in *ld/ld* limb buds (Fig. 3b,f, see also Haramis et al., 1995). However, in limb buds of both *Xt/Xt* (Fig. 3c,g) and *Xt;ld* double homozygous embryos (Fig. 3d,h) posterior restriction and characteristic nesting of the early *Hoxd11* and *Hoxd13* domains are completely lost. No significant differences are observed between *Xt/Xt* and *Xt;ld* double homozygous limb buds (compare Fig. 3c,g to 3d,h; *Hoxd12*, data not shown), establishing that *Gli3*-mediated repression controls posterior nesting of 5′HoxD genes independent of *formin*. Furthermore, no striking changes of 5′HoxD distributions are observed in the posterior trunk of *Gli3*-deficient embryos, indicating that colinear activation of 5′HoxD genes is not affected (data not shown).

Gli3- and *formin*-mediated interactions regulate aspects of the transition from early to late 5′HoxD domains, but not of the spatial distribution of 5′HoxA paralogues

During subsequent limb-bud patterning, the 5′HoxD domains expand anteriorly and restrict distally in wild-type limb buds (transition to the 'late domains') as shown for *Hoxd11* in Fig. 4a. As previously reported, this anterior expansion of 5′HoxD domains is delayed in *ld/ld* limb buds (Fig. 4b; for details see Haramis et al., 1995). Despite of the complete loss in initial posterior nesting (Fig. 3), distal restriction still occurs in the medial mesenchyme of *Xt/Xt* limb buds (arrow, Fig. 4c), giving the late 5′HoxD domains their U-shaped appearance (compare Fig. 4c to Fig. 3c for *Hoxd11* and data not shown). In contrast, aberrant expression of the three 5′ most HoxD genes (*Hoxd11* to *Hoxd13*) persists in the proximal limb-bud mesenchyme of *Xt;ld* double mutant embryos (*Hoxd11*: arrow, Fig. 4d; *Hoxd12* and *Hoxd13*, data not shown). Furthermore, the spatial distributions of 5′HoxD genes in *Xt/Xt* limb buds (Figs 3c,g, 4c) are reminiscent of the ones of their HoxA paralogues, which are expressed without anteroposterior, but with proximodistal restriction in wild-type limb buds (see e.g. Nelson et al., 1996). In particular, comparison of the *Hoxd11* domain in *Xt/Xt* limb buds (Fig. 4c) to the *Hoxa11* domain in wild-type limb buds (Fig. 4e) reveals the apparent similarity of their distributions during the transition from early to late domains. Furthermore, no changes are detected in the characteristic proximodistal restriction of 5′HoxA genes as the distributions of *Hoxa11* and *Hoxa13* transcripts are very similar between wild-type (Fig. 4e,g), *Xt/Xt* (Fig. 4f and data not shown) and *Xt;ld* double mutant limb buds (Fig. 4h and data not shown) during the same developmental period.

Gli3 and *formin* are part of the genetic mechanism that positions and upregulates the *Shh* expression domain at the posterior limb-bud margin

Deregulated 5′HoxD expression (Figs 3, 4) and disrupted autopod morphogenesis (Fig. 2) might reflect underlying defects in anteroposterior polarisation of the limb field and/or establishment of the polarising region. To detect possible alterations in initial limb field polarization, the *Hoxb8* distribution was studied in all relevant genotypes during onset of forelimb-bud outgrowth (Fig. 5a-d). No significant differences were observed by comparing wild-type (Fig. 5a) to either single (Fig. 5b,c) or *Xt;ld* double homozygous forelimb buds (Fig. 5d). *Hoxb8* expression within the posterior compartment always extends to medial, but never anterior mesenchyme (arrowheads, Fig. 5a-d). During limb-bud emergence, *Shh* expression is activated by the mesenchymal cells of the polarising region, which are initially located at the posterior limb-bud margin (Riddle et al., 1993). In *Xt/Xt* limb buds, *Shh* expression is correctly initiated and upregulated to normal levels at the posterior limb-bud margin (Fig. 5e and data not shown) and weak ectopic anterior *Shh* expression is only apparent much later (around embryonic day 11 in forelimb buds, data not shown; for details see Masuya et al., 1995; Buescher et al., 1997). Activation and initial positioning of *Shh* is also normal in *ld/ld* limb buds (Fig. 5f), but subsequent upregulation and distal propagation of the *Shh* domain are disrupted (for details see Introduction). In contrast, *Shh* transcripts are barely or not at all detectable in most *Xt;ld* double homozygous limb buds analyzed. In fact, the limb buds shown in Fig. 5g,h are representative of the highest *Shh* levels detected by embryonic day 10.25 (32 to 34 somites). Most strikingly, *Shh* transcripts are not detected at the posterior limb-bud margin, but at variable subapical positions within the posterior half of the limb-bud mesenchyme (compare Fig. 5g to 5e,f) and are often displaced to the apex (Figs 5h, 6d; 5 of 10 embryos). However, *Shh* expression was never detected in the anterior half of the limb-bud mesenchyme. In addition, *Fgf-4* is not expressed and *Fgf-8* levels are reduced in *Xt;ld* double mutant AERs (data

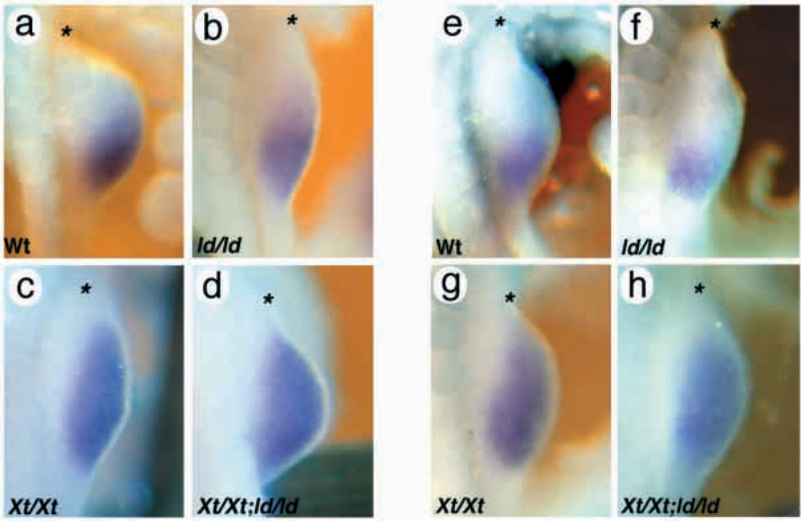

Fig. 3. Establishment of the posteriorly nested 5′HoxD expression domains during initiation of limb-bud outgrowth. (a-h) Forelimb buds of embryonic day 9.75 (28 somites) were hybridized with riboprobes to detect *Hoxd11* (a-d) and *Hoxd13* transcripts (e-h, contralateral limb buds). Asterisks mark the anterior margins of limb buds. (a,b) *Hoxd11* is posteriorly restricted in wild-type (a) and *ld/ld* (b) limb buds. (c,d) Posterior restriction of *Hoxd11* is lost in *Xt/Xt* (c) and *Xt;ld* double homozygous (d) limb buds. (e,f) *Hoxd13* expression in wild-type (e) and *ld/ld* (f) limb buds. Note that the *Hoxd13* domain is smaller than the *Hoxd11* domain in the contralateral limb bud (revealing posterior nesting). (g,h) Posterior restriction of *Hoxd13* is lost in *Xt/Xt* (g) and in *Xt;ld* double homozygous limb buds (h).

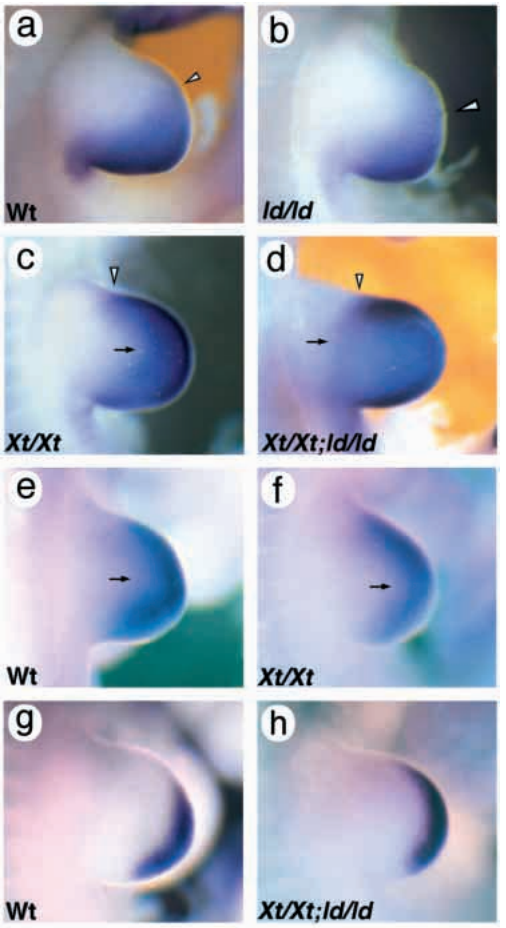

Fig. 4. Transition from early to late *Hoxd11* domains and comparison to 5′HoxA distributions. (a-d) *Hoxd11* distribution in forelimb buds during embryonic day 10.75 (36-39 somites). Arrowheads indicate the anterior limits of the *Hoxd11* expression domains. (a) Wild-type forelimb bud to show the anterior expansion and distal restriction of the *Hoxd11* domain. (b) *ld/ld* forelimb bud to show the delay in anterior expansion of the *Hoxd11* domain. (c) *Xt/Xt* forelimb bud. *Hoxd11* restricts distally within the limb-bud mesenchymal core (arrow). (d) *Xt;ld* double homozygous forelimb bud. Significant *Hoxd11* expression remains proximal (arrow). (e,f) *Hoxa11* expression in forelimb buds (36-37 somites). (e) Wild-type forelimb bud, *Hoxa11* expression is distally restricted but shows no anteroposterior preference. (f) *Xt/Xt* forelimb bud, the shape of the *Hoxa11* domain looks similar to its wild-type counterpart shown in e. Arrows in c-f indicate the extent of distal restriction within the core mesenchyme. (g,h) *Hoxa13* expression in forelimb buds (36-37 somites). (g) Wild-type forelimb bud, *Hoxa13* expression is more distally restricted than *Hoxa11* (compare to e). (h) *Xt;ld* double homozygous forelimb bud. Note the similarity to the wild-type distribution shown in g.

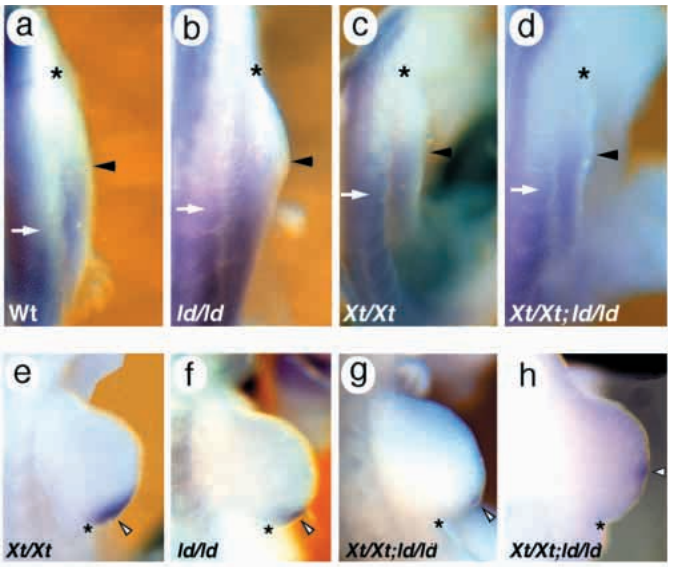

Fig. 5. Transfer of polarizing activity from the limb field to the limb bud. (a-d) Limb field polarization is normal as evidenced by comparative analysis of *Hoxb8* distributions during initiation of forelimb-bud outgrowth (embryonic day 9.25, 23-25 somites). Anterior boundaries of *Hoxb8* expression in the limb-bud and somitic mesoderm are indicated by black arrowheads and white arrows, respectively. Asterisks indicate the anterior margins of the emerging forelimb buds. (a) Wild-type forelimb. (b) *ld/ld* forelimb bud. (c) *Xt/Xt* forelimb bud. (d) *Xt;ld* double homozygous forelimb bud. Note: all embryos are age-matched, but the slight variations in limb-bud size are due to slight variations in outgrowth at this stage and not linked to the genotype. *Hoxb8* expression is restricted to the posterior half of all limb buds. Expression in limb buds is shifted about 1.5 to 2 somites more anterior in comparison to the trunk. (e-h) Positioning and upregulation of the *Shh* domain is disrupted in *Xt;ld* double homozygous limb buds as shown by analysis of forelimb buds (embryonic day 10.25, 32-34 somites). Asterisks mark the posterior margins of limb buds; white arrowheads marks the anterior expression boundary of *Hoxb8* in somites. (e) *Xt/Xt* forelimb bud. At this developmental stage, *Shh* expression is indistinguishable from wild-type limb buds (data not shown). (f) *ld/ld* forelimb bud, *Shh* expression is activated at the posterior margin, but not upregulated. (g,h), *Xt;ld* double mutant forelimb buds showing low *Shh* expression either more posteriorly (g) or mispositioned to the limb-bud apex (h; 5 of 10 embryos). The examples shown in g and (h) are among the *Xt;ld* double homozygous embryos with highest levels of *Shh* transcripts in limb buds. *Shh* levels were much lower or not detectable in most other *Xt;ld* double homozygous limb buds and could not reliably be detected before embryonic day 10.25 (data not shown).

not shown) as previously described for *ld/ld* mutant AERs (Chan et al., 1995; Haramis et al., 1995; Kuhlman and Niswander, 1997).

Transcriptional activation of two mesenchymal targets of SHH signaling, *Ptc* and *Gli* (Marigo et al., 1996; Platt et al., 1997) was analyzed to determine whether low and/or displaced *Shh* expression results in transduction of a signal indicative of polarizing activity. These studies showed that transcription of *Ptc* is never significantly upregulated in *Xt;ld* double homozygous limb buds in contrast to single mutant and wild-type embryos (data not shown). However, *Shh* expression either more posterior (Fig. 6c) or apical (Fig. 6d) induces *Gli* transcription (Fig. 6g,h) as shown by comparative analysis of contralateral *Xt;ld* double homozygous limb buds. As in wild-type (Platt et al., 1997) and single mutant limb buds (Fig. 6e,f), *Gli* transcription is induced in mesenchymal cells responding to the SHH signal (compare e.g. Fig. 6a to e and Fig. 6d to h). However, *Gli* transcript levels are always lower in *Xt;ld* double mutant limb buds in comparison to their wild-type (data not shown) and single mutant counterparts (compare Fig. 6g,h to e,f).

DISCUSSION

Gli3 (Xt) and *formin (ld)* interact genetically during limb pattern formation

Our studies establish that *Gli3* and *formin* interact during limb morphogenesis. Firstly, both proximal (humerus and scapula) and distal (digits) limb skeletal elements are more severely affected in *Xt;ld* double than single homozygous limb buds. Secondly, molecular analysis shows that both positioning of the *Shh*-expressing polarising region and spatial regulation 5′HoxD domains are disrupted in *Xt;ld* double mutant limb buds. As *Gli3* and *formin* are co-expressed in the posterior limb-bud mesenchyme (Fig. 7b; for details see Trumpp et al., 1992; Chan et al., 1995; Masuya et al., 1997), these two proteins with postulated nuclear functions (Chan and Leder, 1996; Marine et al., 1997) might directly interact. However, biochemical studies using cultured embryonic fibroblasts co-expressing epitope-tagged *Gli3* and *formin* proteins failed to provide any evidence for direct molecular interactions (data not shown). Therefore, the molecular and phenotypic alterations observed in *Xt;ld* double mutant limb buds are most likely caused by disruption of two distinct, but genetically interacting cascades. Presently, it is not known at what level these cascades are disrupted by the *Xt* mutation, but *formin* participates in these genetic interactions most likely through its primary function in establishing the SHH/FGF-4 feedback loop (as indicated by the green loop in Fig. 7; for details see Introduction).

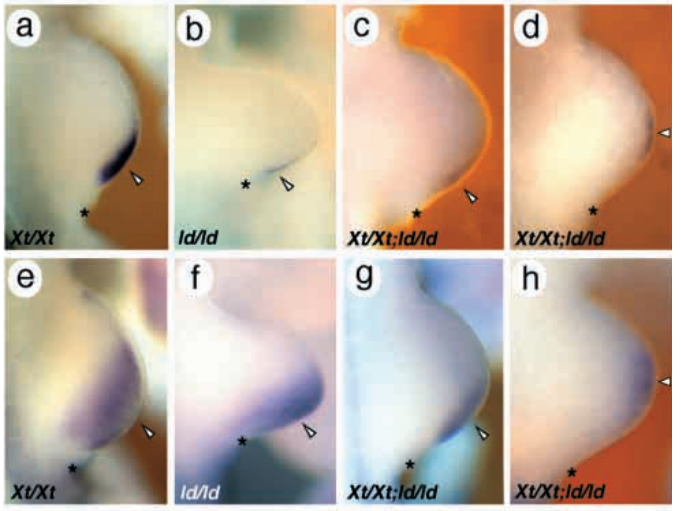

Fig. 6. Transcriptional activation of *Gli* in limb-bud mesenchymal cells responding to SHH signaling. Comparative analysis of *Shh* (a-d) and *Gli* (e-h) distributions in contralateral hindlimb buds of embryos at embryonic day 11 (about 40 somites). Arrowheads indicate either the *Shh* or *Gli* expression domains and asterisks mark posterior limb-bud margins. (a) *Xt/Xt*, *Shh* expression is comparable to wild-type hindlimb buds at this developmental stage (data not shown). (b) *ld/ld*, *Shh* expression remains proximal at low levels. Note that the *ld* phenotype is already apparent in hindlimb buds at this developmental stage. (c) *Xt;ld* double homozygous hindlimb bud with posterior *Shh* expression. (d) *Xt;ld* double homozygous hindlimb bud with apical *Shh* expression. (e-h) *Gli* expression in contralateral hindlimb buds of the same embryos as shown in a-d. Note that *Gli* expression is highest in cells close to the *Shh* domain. (e) *Xt/Xt* hindlimb bud. (f) *ld/ld* hindlimb bud. (g) *Xt;ld* double homozygous hindlimb bud with posterior *Gli* expression. (h) *Xt;ld* double homozygous hindlimb bud with apical *Gli* expression.

Fig. 7 summarizes the *Gli3*- and *formin*-mediated interactions in correlation with their respective distributions during early limb-bud outgrowth. During initiation of limb-bud outgrowth, mesenchymal cells activate *Gli3* expression (Fig. 7a; Masuya et al., 1997) and *Gli3*, but not *formin*, is essential to posteriorly restrict the early 5′HoxD domains (Fig. 7a, upper right). In contrast to *Gli3*, *formin* is initially predominantly expressed by the AER (Fig. 7a; Trumpp et al., 1992; Chan et al., 1995), but expression in the posterior limb-bud mesenchyme is upregulated during early limb-bud outgrowth (Fig. 7b; for details see Trumpp et al., 1992). Firstly, correct positioning and establishment of the *Shh*-expressing polarising region at the posterior limb-bud margin depends on a genetic synergism involving both *Gli3* and *formin* (Fig. 7b, upper left). Secondly, *Gli3*- and *formin*-mediated interactions regulate aspects of the coordinated spatial restriction during the transition from early to late 5′HoxD domains (Fig. 7b, upper right). The ectopic proximal 5′HoxD expression in *Xt;ld* double mutant limb buds provides a likely molecular explanation for the observed defects in proximal skeletal elements as ectopic 5′HoxD expression is known to induce truncations (Goff and Tabin, 1997; Hérault et al., 1997; Peichel et al., 1997). Finally, the rudimentary autopods of *Xt;ld* double homozygous limbs are probably a consequence of the combined effects of low levels of aberrant SHH signaling and deregulated 5′HoxD expression, as these gene products are essential for morphogenesis of distal limb structures (see Introduction and below).

Formin and *Gli3* are part of the genetic mechanism that establishes the *Shh*-expressing polarising region at the posterior limb-bud margin

Low levels of polarizing activity are already established in the posterior half of the limb field (Hornbruch and Wolpert, 1991) and is defined by the *Hoxb8* expression domain in the forelimb field (Fig. 7a; upper left, green area; Charité et al., 1994; Lu et al., 1997; Stratford et al., 1997). In particular, *Hoxb8* seems to be one of possibly several mesenchymal factors that establish competence to induce *Shh* expression in the posterior limb-bud mesenchyme (Fig. 7b; upper left, green area) as ectopic anterior *Hoxb8* expression results in establishment of an ectopic anterior SHH domain (Charité et al., 1994). Interestingly, *Hoxb8* expression is normal in *Xt;ld* double homozygous limb buds and the observed low levels of *Shh* transcripts are always confined to the posterior half of the limb-bud mesenchyme. These results suggest that limb field polarisation and competence to induce *Shh* expression are not affected in *Xt;ld* double mutant limb buds. In addition, the involvement of a positively acting AER signal has been postulated to restrict *Shh* activation to the subapical mesenchyme (Fig. 7b; upper left, yellow area; Helms et al., 1996) and FGF-8 signaling has been implicated in *Shh* activation (Grieshammer et al., 1996; Ros et al., 1996). Indeed, the low levels of aberrant *Shh* expression detected in *Xt;ld* double homozygous limb buds are always restricted to mesenchymal cells in close proximity to the AER. Most relevant to the present study, polarising activity is restricted to a group of mesenchymal cells located at the posterior limb-bud margin during initiation of limb-bud outgrowth. These cells

begin to express the SHH signaling molecule and define the polarising region (Fig. 7b; upper left, purple area; Hornbruch and Wolpert, 1991; Riddle et al., 1993). Our studies establish that *Gli3*- and *formin*-mediated positive feedback regulation of *Shh* expression are both required to stably position the polarising region at the posterior limb-bud margin. Subsequent maintenance and distal propagation of SHH signaling depends on mesenchymal *formin*, as the SHH/FGF-4 feedback loop is never established in *ld/ld* limb buds (Fig. 7b; panel 'Limb Patterning,' Chan et al., 1995; Haramis et al., 1995; Kuhlman and Niswander, 1997). In addition, signals specifying dorsoventral limb fates (reviewed by Zeller and Duboule, 1997) also participate in establishment and maintenance of SHH signaling, which indicates its coordinated spatial regulation along all three limb-bud axes. For example, mice deficient for the dorsalizing *Wnt-7a* signaling molecule also display reduced *Shh* levels and associated patterning defects of distal limb skeletal elements (Parr and McMahon, 1995).

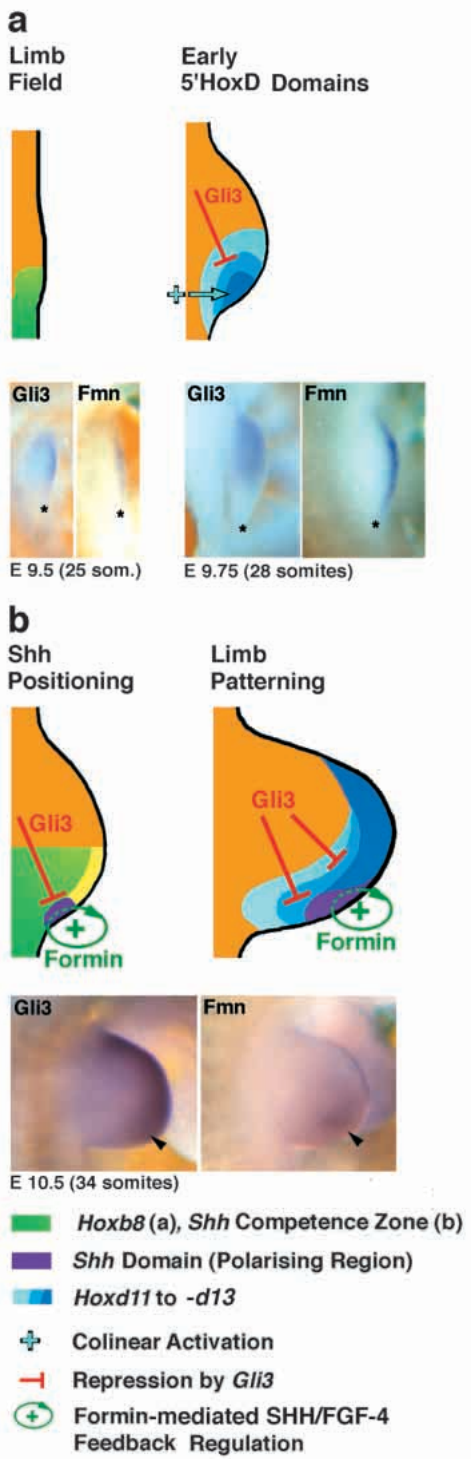

Initial posterior restriction of 5′HoxD domains in limb buds depends on transacting *Gli3*, whereas subsequent regulation requires both *Gli3* and *formin*

Considering previous studies (Masuya et al., 1995; Buescher et al., 1997), one unexpected finding of the present study is that *Gli3* functions first to posteriorly restrict 5′HoxD genes (*Hoxd11* to *Hoxd13*). These results show that their characteristic posterior nesting is not only dependent on successive activation (reviewed by Duboule, 1992), but on *Gli3*-mediated anterior repression during initiation of limb-bud outgrowth (Fig. 7a, panel '5′HoxD'). *Gli3* belongs to a family of zinc finger proteins and analysis of *Xenopus laevis Gli3* indicates that it can act as a transcriptional repressor (Marine et al., 1997). Therefore, *Gli3* could mediate repression by direct binding to *cis*-acting negative regulatory HoxD elements. Indeed, identification of several such negative

Fig. 7. *Gli3* and *formin* are part of a genetic network regulating establishment and propagation of posterior limb-bud identity. (a) Limb field polarisation and establishment of the early 5′HoxD domains. (a; upper left) *Hoxb8* marks polarising activity in the forelimb field and defines initial competence to induce *Shh* expression (green, Charité et al., 1994). These early determinative steps precede both *Gli3* and *formin* functions in establishment of the polarising region. (a; upper right) Establishment of posterior identity during onset of limb-bud outgrowth results in posterior nesting of the 5′HoxD domains. Colinear activation (Duboule, 1992) together with *Gli3*-mediated repression controls posterior restriction of 5′HoxD domains independent of *formin*. (a; lower panels) Distribution of *Gli3* and *formin* (Fmn) during early forelimb-bud outgrowth in wild-type embryos (left panels: embryonic day 9.5, 25 somites; right panels: embryonic day 9.75, 28 somites; for details see Trumpp et al., 1992; Masuya et al., 1997). Asterisks mark the posterior limb-bud margins. (b) Synergistic genetic interaction of *Gli3* and *formin* participates in positioning of the polarising region and regulation of the spatial distribution of 5′HoxD genes. (b; upper left) During initiation of limb-bud outgrowth, *Shh* expression is induced by mesenchymal cells located at the posterior limb-bud margin (thereby defining the polarising region, Riddle et al., 1993). The competence to express *Shh* (green, marked by *Hoxb8*) is limited to subapical mesenchymal cells (yellow) by a positively acting AER factor, which could be FGF-8 (Grieshammer et al., 1996; Ros et al., 1996). *Shh* activation is restricted to the polarising region (purple) by synergistic interaction of *Gli3* and *formin.* In particular, *formin* is essential for establishment of the positive SHH/FGF-4 feedback loop (Chan et al., 1995; Haramis et al., 1995; Kuhlman and Niswander, 1997). (b; upper right) The posterior position of the polarising region is maintained by continued interactions during upregulation and distal propagation of SHH signaling. *Gli3*- and *formin*-mediated interactions also function in the coordinated distal restriction and anterior expansion of the late 5′HoxD domains. (b; lower panels) *Gli3* and *formin* (Fmn) are co-expressed in the posterior limb-bud mesenchyme (arrowheads). Shown are wild-type forelimb buds at embryonic day 10.5 (34 somites).

regulatory elements within or close to the HoxD gene cluster has revealed the importance of transcriptional repression in shaping of their expression domains (van der Hoeven et al., 1996; Hérault et al., 1997; Peichel et al., 1997; Kondo et al., 1998).

Interestingly, deregulation of 5′HoxD expression in *Xt/Xt* limb buds (by embryonic day 9.5; this study) long precedes detection of weak anterior ectopic SHH signalling and activation of its downstream targets *Ptc* and *Gli* (around embryonic day 11; Masuya et al., 1995 Buescher et al., 1997 and data not shown). Therefore, it is rather unlikely that deregulated anterior 5′HoxD expression in *Xt/Xt* limb buds is a consequence of ectopic SHH signaling as previously proposed (Masuya et al., 1995; Buescher et al., 1997). On the contrary, the ectopic *Shh* induction in *Xt/Xt* limb buds might rather be a consequence of deregulated 5′HoxD expression as transgene-mediated ectopic *Hoxd12* expression in wild-type limb buds also results in establishment of an anterior SHH signaling domain and digit polydactyly (Knezevic et al., 1997). The analysis of several other polydactylous mouse mutations has begun to uncover an ‘anterior negative regulatory’ cascade (reviewed by Johnson and Tabin, 1997), which might regulate aspects of 5′HoxD distributions and/or polarizing activity in concert with/or independent of *Gli3*. For example, inactivation of the *Alx-4* gene by gene targeting (Qu et al., 1997) or *lst* mutations in the mouse (Qu et al., 1998) also results in preaxial polydactyly and anterior SHH signaling in older limb buds. The de novo induction of a well-separated, anterior *Hoxd13* domain together with normal *Gli3* expression in *Alx-4*-deficient limb buds (and vice-versa) suggests that *Alx-4* acts either downstream or independent of *Gli3*. However, genetic evidence also indicates that wild-type *formin* function is required for the semidominant, polydactylous *lst* limb phenotype (Vogt and Leder, 1996).

The results of this study indicate that *Gli3*- and *formin*-mediated signalling interactions regulate aspects of the dynamic spatial distributions of 5′HoxD genes, which result in the temporally and spatially coordinated establishment of their late expression domains during progression of limb-bud development. Genetic and evolutionary evidence indicates that the late 5′HoxD domains are essential for formation and patterning of the vertebrate autopod (see e.g. Dollé et al., 1993; Sordino et al., 1995). The deregulated expression of 5′HoxD genes in both single and *Xt;ld* double homozygous limb buds provides a likely direct molecular explanation for the observed digit patterning defects (see also Haramis et al., 1995; Masuya et al., 1995; Buescher et al., 1997). Furthermore, the expression of paralogous 5′HoxA genes is apparently normal in both single and *Xt;ld* double homozygous limb buds, indicating that *Gli3*- and *formin*-mediated genetic interactions regulate specifically the limb-bud domains of 5′HoxD genes. Therefore, these observations might have evolutionary relevance as differential expression of paralogous Hox genes has been proposed as important during evolution of paired appendages (reviewed by Shubin et al., 1997; Coates and Cohn, 1998).

We thank U. Rüther and D. Büscher for providing the first generation of Xt^H and Xt^J mice, probes and oligos for genotyping. We are grateful to J. Deschamps (*Hoxb8*), P. Dollé and S. Potter (*Hoxa*), D. Duboule (*Hoxd*), C. C. Hui (Gli), A. McMahon (*Shh*) and U. Rüther (*Ptc* and *Gli3*) for providing probes for in situ analysis. A. Haramis, A. Trumpp and T. Schimmang are thanked for many stimulating discussions, and for providing mice and reagents. We thank T. Bouwmeester, S. Chabanis, G. Davidson, J. Deschamps, R. Dono, C. McGuigan, I. Mattaj and C. Niehrs for comments on the manuscript. This work was supported by EMBL, EU-grant CI1*CT93-0017 and a Fellowship of the Graduiertenkolleg ‘Experimentelle Nieren- und Kreislaufforschung’ (University of Heidelberg) to A. Z.

REFERENCES

Biesecker, L. (1997). Strike three for GLI3. *Nat. Genet.* **17**, 259-260.

Buescher, D., Bosse, B., Heymer, J. and Ruether, U. (1997). Evidence for genetic control of *Sonic hedgehog* by *Gli3* in mouse limb development. *Mech. Dev.* **62**, 175-182.

Chan, D. C., Wynshaw-Boris, A. and Leder, P. (1995). Formin isoforms are differentially expressed in the mouse embryo and are required for normal expression of *fgf-4* and *shh* in the limb bud. *Development* **121**, 3151-3162.

Chan, D. C. and Leder, P. (1996). Genetic evidence that formins function within the nucleus. *J. Biol. Chem.* **271**, 23472-23477.

Charité, J., de Graaff, W., Shen, S. and Deschamps, J. (1994). Ectopic Expression of Hoxb-8 Causes Duplication of the ZPA in the Forelimb and Homeotic Transformation of Axial Structures. *Cell* **78**, 589-601.

Chiang, C., Litingtung, Y., Lee, E., Young, K. E., Corden, J. L., Westphal, H. and Beachy, P. A. (1996). Cyclopia and defective axial patterning in mice lacking *Sonic hedgehog* gene function. *Nature* **383**, 407-413.

Coates, M. I. and Cohn, M. J. (1998). Fins, limbs, and tails: outgrowths and axial patterning in vertebrate evolution. *BioEssays* **20**, 371-381.

Cohn, M. J. and Tickle, C. (1996). Limbs: a model for pattern formation within the vertebrate body plan. *Trends Genet.* **12**, 253-257.

Cohn, M. J., Patel, K., Krumlauf, R., Wilkinson, D. G., Clarke, J. D. W. and Tickle, C. (1997). *Hox9* genes and vertebrate limb specification. *Nature* **387**, 97-101.

Dollé, P., Izpisua-Belmonte, J. C., Falkenstein, H., Renucci, A. and Duboule, D. (1989). Coordinate expression of the murine Hox-5 complex homeobox-containing genes during limb pattern formation. *Nature* **342**, 767-772.

Dollé, P., Dietrich, A., LeMeur, M., Schimmang, T., Schuhbaur, B., Chambon, P. and Duboule, D. (1993). Disruption of the Hoxd-13 gene induces localized heterochrony leading to mice with neotenic limbs. *Cell* **75**, 431-441

Duboule, D. (1992). The vertebrate limb: a model system to study the HOX/HOM gene network during development and evolution. *BioEssays* **14**, 375-384.

Duboule, D. (1995). Vertebrate Hox genes and proliferation: an alternative pathway to homeosis? *Curr. Opin. Genet. Dev.* **5**, 525-528.

Echelard, Y., Epstein, D. J., St-Jacques, B., Shen, L., Mohler, J., McMahon, J. A. and McMahon, A. P. (1993). Sonic Hedgehog, a member of a family of putative signaling molecules, is implicated in the regulation of CNS polarity. *Cell* **75**, 1417-1430.

Goff, D. J. and Tabin, C. J. (1997). Analysis of *Hoxd-13* and *Hoxd-11* misexpression in chick limb buds reveals that *Hox* genes affect both bone condensation and growth. *Development* **124**, 627-636.

Grieshammer, U., Minowada, G., Pisenti, J. M., Abbott, U. K. and Martin, G. R. (1996). The chick *limbless* mutation causes abnormalities in limb bud dorsal-ventral patterning: implications for the mechanism of apical ridge formation. *Development* **122**, 3851-3861.

Haramis, A. G., Brown, J. M. and Zeller, R. (1995). The limb deformity mutation disrupts the SHH/FGF-4 feedback loop and regulation of 5′HoxD genes during limb pattern formation. *Development* **121**, 4237-4245.

Helms, J., Kim, C., Thaller, C. and Eichele, G. (1996). Retinoic acid signalling is required during early limb bud development. *Development* **122**, 1385-1394.

Hérault, Y., Fraudeau, N., Zakany, J. and Duboule, D. (1997). *Ulnaless* (*Ul*), a regulatory mutation inducing both loss-of-function and gain-of-function of posterior Hoxd genes. *Development* **124**, 3493-3500.

Hornbruch, A. and Wolpert, L. (1991). The spatial and temporal distribution of polarizing activity in the flank of the pre-limb-bud stages in the chick embryo. *Development* **111**, 725-731.

Hui, C.C. and Joyner, A. (1993). A mouse model of greig cephalopolysyndactyly syndrome: the extra-toesJ mutation contains an intragenic deletion of the Gli3 gene. *Nat-Genet.* **3**, 241-246.

Hui, C.C., Slusarski, D., Platt, K., Holmgren, R. and Joyner, A. (1994).

Expression of three mouse homologs of the Drosophila segment polarity gene cubitus interruptus, Gli, Gli-2, and Gli-3, in ectoderm- and mesoderm-derived tissues suggests multiple roles during postimplantation development. *Dev. Biol.* **162**, 402-413.

Johnson, D. R. (1967). *Extra-toes*: a new mutant gene causing multiple abnormalities in the mouse. *J. Embryol. Exp. Morph.* **17**, 543-581.

Johnson, R. L. and Tabin, C. J. (1997). Molecular models for vertebrate limb development. *Cell* **90**, 979-990.

Knezevic, V., De Santo, R., Schughart, K., Huffstadt, U., Chiang, C., Mahon, K. A. and Mackem, S. (1997). *Hoxd-12* differentially affects preaxial and postaxial chondrogenic branches in the limb and regulates *Sonic hedgehog* in a positive feedback loop. *Development* **124**, 4523-4536.

Kondo, T., Zakany, J. and Duboule, D. (1998). Control of colinearity in AbdB genes of the mouse HoxD complex. *Mol. Cell* **1**, 289-300.

Kuhlman, J. and Niswander, L. (1997). Limb deformity proteins: role in mesodermal induction of the apical ectodermal ridge. *Development* **124**, 133-139.

Laufer, E., Nelson, C. E., Johnson, R. L., Morgan, B. A. and Tabin, C. (1994). Sonic hedgehog and Fgf-4 act through a signalling cascade and feedback loop to integrate growth and patterning of the development limb bud. *Cell* **79**, 993-1003.

Lu, H. C., Revelli, J. P., Goering, L., Thaller, C. and Eichele, G. (1997). Retinoid signalling is required for the establishment of a ZPA and for the expression of Hoxb-8, a mediator of ZPA formation. *Development* **124**, 1643-1651.

Maas, R. L., Zeller, R., Woychik, R. P., Vogt, T. F. and Leder, P. (1990). Disruption of formin-encoding transcripts in two mutant limb deformity alleles. *Nature* **346**, 853-855.

Marigo, V., Johnson, R. L., Vortkamp, A. and Tabin, C. (1996). Sonic hedgehog Differentially Regulates Expression of *GLI* and *GLI3* during Limb Development. *Dev. Biol.* **180**, 273-283.

Marine, J. C., Bellefroid, E. J., Pendeville, H., Martial, J. A. and Pieler, T. (1997). A role for *Xenopus* Gli-type zinc finger proteins in the early embryonic patterning of mesoderm and neuroectoderm. *Mech. Dev.* **63**, 211-225.

Masuya, H., Tomoko, S., Wakana, S., Moriwaki, K. and Shiroishi, T. (1995). A duplicated zone of polarizing activity in polydactylous mouse mutants. *Genes Dev.* **9**, 1645-1653.

Masuya, H., Sagai, T., Moriwaki, K. and Shiroishi, T. (1997). Multigenic Control of the Localization of the Zone of Polarizing Activity in Limb Morphogenesis in the Mouse. *Dev. Biol.* **182**, 42-51.

Nelson, C. E., Morgan, B. A., Burke, A. C., Laufer, E., DiMambro, E., Murtaugh, L. C., Gonzales, E., Tessarollo, L., Parada, L. F. and Tabin, C. (1996). Analysis of *Hox* gene expression in the chick limb bud. *Development* **122**, 1449-1466.

Niswander, L., Jeffrey, S., Martin, G. R. and Tickle, C. (1994). A positive feedback loop coordinates growth and patterning in the vertebrate limb. *Nature* **371**, 609-612.

Niswander, L. (1997). Limb mutants: what can they tell us about normal limb development? *Curr. Opin. Genet. Dev.* **7,** 530-536.

Parr, B. A. and McMahon, A. P. (1995). Dorsalizing signal Wnt-7a required for normal polarity of D-V and A-P axes of mouse limb. *Nature* **23**, 350-353.

Peichel, C. L., Prabhakaran, B. and Vogt, T. F. (1997). The mouse *Ulnaless* mutation deregulates posterior HoxD gene expression and alters appendicular patterning. *Development* **124**, 3481-3492.

Platt, K. A., Michaud, J. and Joyner, A. L. (1997). Expression of the mouse Gli and Ptc genes is adjacent to embryonic sources of hedgehog signals suggesting a conservation of pathways between flies and mice. *Mech. Dev.* **62**, 121-135.

Qu, S. K., Niswender, Q., Ji, R., van der Meer, D., Keeny, M., Magnuson A., and Wisdom, R. (1997). Polydactyly and ectopic ZPA formation in *Alx-4* mutant mice. *Development* **124**, 3999-4008.

Qu, S., Tucker, S. C., Ehrlich, J. S., Levorse, J. M., Flaherty, L. A., Wisdom, R. and Vogt, T. F. (1998). Mutations in mouse aristaless-like4 cause Strong's luxoid polydactyly. *Development* **125**, 2711-2721.

Riddle, R. D., Johnson, R. L., Laufer, E. and Tabin C. (1993). *Sonic hedgehog* mediates the polarizing activity of the ZPA. *Cell* **75**, 1401-1416.

Ros, M. A., Lopez-Martinez, A., Simandl, B. K., Rodriguez, C., Izpisua Belmonte, J. C., Dahn, R. and Fallon, J. F. (1996). The limb field mesoderm determines initial limb bud anteroposterior asymmetry and budding independent of *sonic hedgehog* or apical ectodermal gene expressions. *Development* **122**, 2319-2330.

Schimmang, T., Lemaistre, M., Vortkamp, A. and Rüther, U. (1992). Expression of the zinc finger gene Gli3 is affected in the morphogenetic mouse mutant extra-toes (Xt). *Development* **116**, 799-804.

Shubin, N., Tabin, C. and Carroll, S. (1997). Fossils, genes and the evolution of animal limbs. *Nature* **388**, 639-647.

Small, K. M. and Potter, S. S. (1993). Homeotic transformations and limb defects in *Hox A11* mutant mice. *Genes Dev.* **7**, 2318-2328.

Sordino, P., van der Hoeven, F. and Duboule, D. (1995). Hox gene expression in teleost fins and the origin of vertebrate digits. *Nature* **375**, 678-681.

Stratford, T. H., Kostakopoulou, K. and Maden, M. (1997). Hoxb-8 has a role in establishing early anterior-posterior polarity in chick forelimb but not hindlimb. *Development* **124**, 4225-4234.

Trumpp, A., Blundell, P. A., de la Pompa, J. L. and Zeller, R. (1992). The chicken *limb deformity* gene encodes nuclear proteins expressed in specific cell types during morphogenesis. *Genes Dev.* **6**, 14-28.

van der Hoeven, F., Zákány, J. and Duboule, D. (1996). Gene transpositions in the *HoxD* complex reveal a hierarchy of regulatory controls. *Cell* **85**, 1025-1035.

Vogt, T. F. and Leder, P. (1996). Polydactyly in the Strong's luxoid mouse is suppressed by limb deformity alleles. *Dev. Genet.* **19**, 33-42.

Woychik, R. P., Stewart, T. A., Davis, L. G., D'Eustachio, P. and Leder, P. (1985). An inherited limb deformity created by insertional mutagenesis in a transgenic mouse. *Nature* **318**, 36-40.

Woychik, R. P., Maas, R. L., Zeller, R., Vogt, T. F. and Leder, P. (1990). 'Formins': Proteins deduced from the alternative transcripts of the limb deformity gene. *Nature* **346**, 850-853.

Wynshaw-Boris, A., Ryan, G., Deng, C. X., Chan, D. C., Jackson-Grusby, L., Larson, D., Dunmore, J. H. and Leder, P. (1997). The role of a single formin isoform in the limb and renal phenotypes of limb deformity. *Mol. Med.* **3**, **372-384.**

Zeller R., Jackson-Grusby, L. and Leder, P. (1989). The limb deformity gene is required for apical ectodermal ridge differentiation and anteroposterior limb pattern formation. *Genes Dev.* **3**, 1481-1492.

Zeller, R. and Duboule, D. (1997). Dorso-ventral limb polarity and origin of the ridge: on the fringe of independence. *BioEssays* **19**, 541-546.